



Donor-to-Donor Heterogeneity in the Clonal Dynamics of Transplanted Human Cord Blood Stem Cells in Murine Xenografts



Mirjam E. Belderbos^{1,2,*}, Sabrina Jacobs¹, Taco K. Koster¹, Albertina Ausema¹, Ellen Weersing¹, Erik Zwart¹, Gerald de Haan¹, Leonid V. Bystriykh¹

¹ Department of Stem Cell Biology and Ageing, European Research Institute for the Biology of Ageing, University of Groningen, Groningen, Netherlands

² Princess Máxima Center for Pediatric Oncology and Oncode Institute, Utrecht, Netherlands

Article history:

Received 1 July 2019

Accepted 26 August 2019

Key Words:

Hematopoietic stem cells

Lineage tracing

Barcode

Heterogeneity

Umbilical cord blood

A B S T R A C T

Umbilical cord blood (UCB) provides an alternative source of hematopoietic stem cells (HSCs) for allogeneic transplantation. Administration of sufficient donor HSCs is critical to restore recipient hematopoiesis and to maintain long-term polyclonal blood formation. However, due to lack of unique markers, the frequency of HSCs among UCB CD34⁺ cells is the subject of ongoing debate, urging for reproducible strategies for their counting. Here, we used cellular barcoding to determine the frequency and clonal dynamics of human UCB HSCs and to determine how data analysis methods affect these parameters. We transplanted lentivirally barcoded CD34⁺ cells from 20 UCB donors into Nod/Scid/IL2Ry^{-/-} (NSG) mice (n = 30). Twelve recipients (of 8 UCB donors) engrafted with >1% GFP⁺ cells, allowing for clonal analysis by multiplexed barcode deep sequencing. Using multiple definitions of clonal diversity and strategies for data filtering, we demonstrate that differences in data analysis can change clonal counts by several orders of magnitude and propose methods to improve their consistency. Using these methods, we show that the frequency of NSG-repopulating cells was low (median ~1 HSC/10⁴ CD34⁺ UCB cells) and could vary up to 10-fold between donors. Clonal patterns in blood became increasingly consistent over time, likely reflecting initial output of transient progenitors, followed by long-term HSCs with stable hierarchies. The majority of long-term clones displayed multilineage output, yet clones with lymphoid- or myeloid-biased output were also observed. Altogether, this study uncovers substantial interdonor and analysis-induced variability in the frequency of UCB CD34⁺ clones that contribute to post-transplant hematopoiesis. As clone tracing is increasingly relevant, we urge for universal and transparent methods to count HSC clones during normal aging and upon transplantation.

© 2019 American Society for Transplantation and Cellular Therapy. Published by Elsevier Inc.

INTRODUCTION

Human umbilical cord blood (UCB) is an established source of hematopoietic stem cells (HSCs) for allogeneic transplantation of patients with a variety of diseases [1]. Compared with other stem cell sources, UCB has the advantages of being readily available and permitting a higher degree of donor-recipient mismatch [1]. However, its main disadvantage is the limited number of cells that can be obtained from a single UCB unit, which may contribute to an increased risk of nonengraftment, delayed hematopoietic recovery, and immune reconstitution [2–5]. Accordingly, HSC content, currently measured as CD34⁺ cells/kg recipient, is a major criterion used to select the optimal UCB unit for transplantation. However, the CD34⁺

population is highly heterogeneous, with few cells fulfilling the (functional) definition of a “true” HSC [6–8]. Accordingly, the frequency of HSCs among the CD34⁺ cell population may vary between different UCB donors, thereby potentially explaining the occurrence of graft failure in patients transplanted with seemingly adequate CD34⁺ HSC doses. Finally, as (age-related) reduction in the number of HSC clones is associated with various adverse health effects, administration of sufficient HSCs may be favorable in the long term as well [9–11]. Altogether, to improve the use of UCB in experimental and clinical transplants, insight into the frequency of HSCs among UCB CD34⁺ cells, their clonal contribution to post-transplant hematopoiesis, and the potential variability in these parameters between individual UCB donors is urgently needed.

Due to lack of unambiguous phenotypic markers, stringent definition of an HSC relies on its capacity to self-renew and to produce robust multilineage progeny. Various experimental methods have been employed, using limiting-dilution transplantation [12], viral integration sites [13,14], genetic barcodes [15,16], fluorescent markers [17–19], CRISPR-Cas9 genome

Financial disclosure: See Acknowledgments on page 24.

* Correspondence and reprint requests: M.E. Belderbos, MD, PhD, Princess Máxima Center for Pediatric Oncology, Heidelberglaan 25, 3584 EA Utrecht, Netherlands.

E-mail address: m.e.belderbos@prinsesmaximacentrum.nl (M.E. Belderbos).

<https://doi.org/10.1016/j.bbmt.2019.08.026>

1083-8791/© 2019 American Society for Transplantation and Cellular Therapy. Published by Elsevier Inc.

editing [20], or Cre-*loxP* recombination [21] to trace the clonal outgrowth of HSCs in unperturbed hematopoiesis or in autologous, syngeneic, or xenogeneic recipients. Using cellular barcodes to count and trace murine LSK48⁺150⁺ hematopoietic stem and progenitor cells (HSPCs) in murine recipients, we previously demonstrated that only a minor fraction of this highly purified population produces clonal offspring and that their quantitative output and lineage commitment are stable over time [15,22]. Similar results have been obtained by other groups, using transplantation of barcoded murine HSPCs in syngeneic recipients [23,24], autologous transplantation of genome-edited HSPCs in nonhuman primates [25,26], or fluorescent markers to trace native hematopoiesis in zebrafish [17]. Regardless of the exact species or experimental model, these studies unequivocally demonstrate that long-term hematopoiesis is maintained by a rare population of cells, with stable multilineage reconstitution over time.

In marked contrast, data on the frequency and lineage commitment of transplanted human HSCs remain scarce and controversial. On one hand, gene therapy studies estimate that 1 in 10⁵ to 10⁶ gene-corrected CD34⁺ HSPCs has the potential to engraft long term and that their lineage commitment is stable for several years after transplantation [14,27]. On the other hand, in vivo lineage tracing studies suggest a considerably higher HSC frequency, indicating that 0.2% of barcoded human CD34⁺ UCB cells produce multilineage progeny upon xenotransplantation in mice, with variable lineage commitment and with the majority of clones only present at a single time point [16]. In addition to obvious differences in the nature of the recipient (human versus murine) and in the employed method to identify and trace HSC clones, this discrepancy could also be due to differences in analytical methods to assess HSC frequency. Besides, as these studies used autologous transplantation [13,14,28] or pooled CD34⁺ cells from >100 donors [16], the interdonor heterogeneity in HSC frequency and lineage commitment remain unknown yet are highly relevant for optimization of HSC transplantation (HSCT) and donor selection protocols.

Here, we have exploited quantitative, high-throughput barcoding technology to characterize the frequency and lineage commitment of CD34⁺ cells from 8 individual human UCB donors and to quantify the potential impact of interdonor and analytical variability on these parameters. We show that the frequency of Nod-SCID-IL2Ry^{-/-} (NSG)-repopulating cells and their lineage contributions differ substantially between human UCB donors, stressing the importance of accurate quantification of graft HSC content. Moreover, we demonstrate that estimates of HSC clone numbers in the same sample can vary several orders of magnitude, depending on the used method of analysis, and we provide guidelines to select the optimal analytical method. Altogether, our findings partially explain some of the discrepancies in HSC frequency in previous studies and urge for uniform and transparent data analysis methods to count HSC clones during normal aging and upon transplantation.

METHODS

Data-Sharing Statement

We adhere to the recent consensus of the StemCellMathLab for utility and reproducibility of clonal tracking studies [29]. Accordingly, data tables containing all raw barcode data included in this study are publicly available through the online repository (Supplementary Table S1).

Barcode Library

The barcode library used for the current studies was described in detail previously [30,31]. Briefly, we cloned synthetic random barcode sequences with 2

similar backbones, AGNNACNNNGTNNCGNNNTANNCCANNNTGNNNGAC or GAANNACNNNGTNNCGNNNTANNCCANNNTAAGGACG, in the modified pGIPZ lentiviral vector and collected over 800 individual DNA-preps and *Escherichia coli* stocks [30,31]. These preps were then pooled at equimolar concentrations to generate the 800-barcode libraries used to transduce target cells, with conventional lentiviral transduction protocols with p 8.91 cytomegalovirus and Vesicular stomatitis virus G-protein viral plasmids [32].

Cord Blood CD34⁺ Cell Isolation, Transduction, and Xenotransplantation

UCB was collected from 20 individual donors, directly after uncomplicated vaginal delivery, using citrate phosphate dextrose-containing collection bags (MacoPharma, Utrecht, Netherlands), according to procedures approved by the Medical Ethical Committee of the University of Groningen. CD34⁺ HSPCs were isolated within 24 hours after birth by Ficoll gradient centrifugation (Sigma Aldrich, Zwijndrecht, Netherlands) and subsequent positive selection using CD34-magnetic beads (Miltenyi, Leiden, Netherlands). Two types of culture medium were used to maintain UCB-derived CD34⁺ HSPCs throughout the transduction procedure: StemSpan supplemented with recombinant human thrombopoietin (recombinant human thrombopoietin (rhTPO), 100 ng/mL; Preprotech, London, UK), stem cell factor (100 ng/mL; R&D Systems, Minneapolis, MN) and FLT3-ligand (100 ng/mL; R&D Systems, UCB donors 1 to 3), or StemSpan supplemented with recombinant human Stem Cell Factor (10 ng/mL), rhTPO (20 ng/mL), Insulin-like growth factor-2 (20 ng/mL; R&D Systems), and recombinant human fibroblast growth factor (10 ng/mL; Preprotech, UCB donors 4 to 20). The type of medium did not have a significant impact on the kinetics of engraftment or on the number of HSC clones (data not shown). UCB CD34⁺ HSPCs were transduced with the lentiviral barcode library for 24 hours in vitro, after which the cells were washed and cultured for another 24 hours. After a total duration of 48 hours, cells were counted using trypan blue, and transduction efficiency was assessed by flow cytometry for green fluorescent protein (GFP). Cells were subsequently transplanted in bulk in sublethally irradiated NSG mice (n = 30, 1 to 2 Gy) with a minimum dose of 1.0 × 10⁵ CD34⁺GFP⁺ cells/recipient.

Detection of Human Blood Cells in Murine Xenografts

Human chimerism and lineage differentiation were monitored in mouse blood at selected time points after transplantation and in bone marrow and spleen at sacrifice. Single-cell suspensions were prepared as described previously [15,30]. Differential blood counts were performed on a Medonic CA620 Hematology Analyzer (Boule Medical AB, Spanga, Sweden). Flow cytometry was used to identify human B cells (hCD45⁺hCD19⁺), T cells (hCD45⁺hCD3⁺), and granulocytes (FSC/SSC high, hCD45⁺hCD16⁺) and the presence of the barcode vector (GFP⁺). Engraftment for each lineage was defined as ≥1% fluorophore-positive cells among total live peripheral blood mononuclear cells [32]. Lineage-sorted cell fractions were obtained using a MoFlo flow cytometer (Beckman Coulter, Woerden, Netherlands), employing the same markers as for flow cytometry.

DNA Isolation and Barcode Sequencing

Genomic DNA was isolated from unsorted cells and sorted cell populations (Supplementary Table S1) using the DNeasy Blood&Tissue Kit (Qiagen, Venlo, Netherlands), according to the manufacturer's instructions. For samples with low cell numbers (blood), the DNA micro kit was used (Qiagen). Barcode sequences were amplified in a 35-cycle PCR reaction using primers for the flanking EGFP (forward) and WPRE (reverse) sites and sequenced in multiplex format on an Illumina HiSeq 2500 Platform (BaseClear, Leiden, Netherlands), as described previously [30,31].

Data Analysis

Barcode sequence extraction, noise filtering, and data processing were performed as previously described [30,31]. Briefly, all unique sequences were first collapsed with the script provided on Github (<https://github.com/erikzwart/collapse-multiplex-barcodes>). Subsequently, unique sequences were demultiplexed by primer tag and split among experiments. Barcode sequences were extracted using custom scripts searching for the barcode backbone motif. Highly similar barcodes were merged using a Hamming distance threshold of ≥1. The resulting list of barcode reads per sample was grouped in tables per experiment. All these tables are available in the supplementary files. Consistency in barcode patterns was expressed as Spearman correlation. Differences between groups were calculated using the Mann-Whitney *U* test for non-normally distributed variables (eg, consistency in barcode patterns over time) or the Student *t* test for normally distributed variables. Paired measurements (eg, the number of barcodes in blood versus bone marrow) were compared using the Wilcoxon signed rank test.

Definitions and Calculation of Barcode Diversity

We used and compared different parameters to assess the diversity of the retrieved barcodes. The first and most simple is *nominal count*, being the number of different barcodes in a given sample.

Second, the *Shannon count* (Sh count) is derived from population dynamics and takes into account both the number of barcodes as well as their relative abundance. The Shannon count for a given sample is determined by first calculating the *Shannon index* (H):

$$H = - \sum_{j=i}^s p_i \ln(p_i)$$

where s is the total number of observed barcodes in a given sample, and p is the proportion of reads belonging to the i th barcode in the sample. The Shannon index is subsequently converted to the Shannon count:

$$Sh_{count} = e^H$$

When all barcodes in a sample are equally distributed, the nominal count and Shannon count are equal, whereas skewed barcode distributions will result in a lower Shannon count (also minimizing its sensitivity to PCR noise) [31].

Third, we calculated several commonly used predictors of population diversity: the abundance-based coverage estimate, the Chao2 estimator, and the Goods completeness coefficient [33,34]. These parameters generally predict total population diversity based on the number of distinct measurements in a given sample, correcting for a certain degree of unseen diversity. For example, the *Chao estimators* are commonly used in ecology and sporadically in gene therapy studies, when it is assumed that only a fraction of the total body “true” clonal diversity is captured in a (blood/bone marrow) sample [34–36]. Chao1 is calculated as

$$S_1 = S_{obs} + \frac{F_1^2}{2F_2}$$

where S_{obs} is the number of species/barcodes, F_1 is the number of singletons, and F_2 is the number of doubletons. Because read frequencies cannot be interpreted in terms of single or double detection of species, we used the Chao2 index, which is conceptually similar to Chao1 but defines single- and doubletons as species/barcodes present only in 1 or 2 samples. All other predictors were defined and calculated using the python scikit-diversity-alpha package (<http://scikit-bio.org/docs/0.5.1/generated/skbio.diversity.alpha.html>).

RESULTS

Barcoded Human Cord Blood CD34⁺ Cells Produce Multilineage Progeny in Murine Xenografts

We set out to quantify the frequency of HSCs and their lineage contribution among different UCB donors. CD34⁺ cells from 20 individual UCB donors were subjected to lentiviral barcoding and transplanted into a total of 30 NSG mice, at a minimum dose of 1.0×10^5 CD34⁺GFP⁺ cells/recipient (Figure 1A, Table 1). In total, 29 recipients engrafted, defined as $\geq 1\%$ human CD45⁺ cells in peripheral blood, at a median interval of 6 weeks (range, 4 to 36) after transplant (Figure 1B–C, Table 1). Of these, 12 recipients (of 8 UCB donors) had sufficient GFP⁺ cells for barcode analysis (Table 1). The kinetics of engraftment varied between leukocyte subtypes: B cells were the most abundant and first to appear at a median time of 10 weeks after transplant (range, 4 to 36), followed by T cells (10 weeks; range, 8 to 42) and myeloid cells (10 weeks; range, 9 to 42; Figure 1D). Ten (34%) mice did not have any human T cell engraftment and 13 (45%) did not have granulocyte engraftment. The interval until human cell engraftment tended to shorten with increasing CD34⁺ cell dose, yet this was not significant (Spearman $\rho = -0.25$, $P = .20$; Figure 1E).

Definitions of Clonal Diversity Affect Several Orders of Magnitude on the Number of Retrieved Clones

Previous studies aimed at counting HSC clones used different definitions of clonal diversity, barcode libraries of varying (known/unknown) sizes, and various analytical methods for data filtering and barcode retrieval [16,17,27,29,36]. To reliably quantify the number of clones in our data, we first assessed the impact of these analytical differences on the number of retrieved HSPCs.

We observed that the log₂-transformed barcode distributions in the barcode library (Figure 2A) and in UCB CD34⁺ cells before transplantation (Figure 2B) were close to normal, reflecting the presence of multiple clones without clonal selection. In contrast, barcode distributions in samples from UCB xenografts showed skewed/bimodal barcode distribution, with a few high-frequency barcodes and many low-frequency reads (representative example in Figure 2C). The first category, high-frequency barcodes, likely contains true clones that survived evolutionary selection, whereas the low-frequency reads will reflect small clones as well as sequencing artifacts. To assess the impact of this distribution on clonal counts, we calculated the number of barcodes in each xenograft, using different definitions of clonal diversity and different thresholds for data filtering. Using nominal counts and unfiltered sequencing results, we found a median of 235 barcodes per xenograft, which were reduced several-fold when data were filtered using increasingly stringent criteria (Figure 2D). In marked contrast, the Shannon count, which incorporates both the number of unique barcodes and their relative abundance, provided a 10-fold lower barcode number, which remained stable across data filtering steps (Figure 2E). To reconcile this apparent paradox, we calculated the clonal diversity in all experiments using different filtering thresholds and estimates of clonal diversity and compared the results with the size of the 800-barcode library (Supplementary Figure S6 and Figure 2F). Theoretically, the cumulative number of barcodes in any experiment should rise asymptotically with repetitive sampling and cannot exceed the size of the library. As expected, the nominal barcode count was always equal to the (arbitrarily defined) filtering threshold (ie, when the top 200 barcodes are filtered, the nominal barcode count is 200). Remarkably, the abundance-based coverage estimate and Chao2 estimators, which predict clonal diversity based on the observed number of barcodes and a certain degree of unseen diversity, reported clonal diversities that were several-fold higher, grew steadily (instead of asymptotically) upon repetitive sampling, and exceeded the size of the library several-fold, likely reflecting their sensitivity to noise. In contrast, the Shannon count reported barcode frequencies that were several-fold lower, remained below the library threshold, and stayed stable throughout data-filtering steps, reflecting its ability to reliably detect major barcode clones. Altogether, this shows that definitions of clonal diversity and thresholds for data filtering can affect clone counts by several-folds magnitude, with the Shannon count being the most consistent and least sensitive to sequencing noise and thus the preferred method. Overall, these findings demonstrate that detailed description of the used data-filtering protocols and methods for clone counting is crucial to assess and compare clonal counts within and across studies.

Interdonor Variability in HSPC Frequency among Cord Blood CD34⁺ Cells

We subsequently used the preferred barcode method to determine the frequency of HSPCs among UCB CD34⁺ cells. Hereto, we longitudinally traced the barcode patterns in blood and bone marrow of GFP⁺ engrafted mice ($n = 12$ recipients of 8 donors) for up to 10 months after transplantation (Table 1). GFP levels in bone marrow varied between recipients and were unrelated to administered cell dose or to pretransplant transduction efficiency (Supplementary Figure S2). Analysis of barcode patterns in longitudinally obtained blood samples identified tens to hundreds of barcodes at each individual time point (Figure 3A,B). Early after transplantation, clone numbers

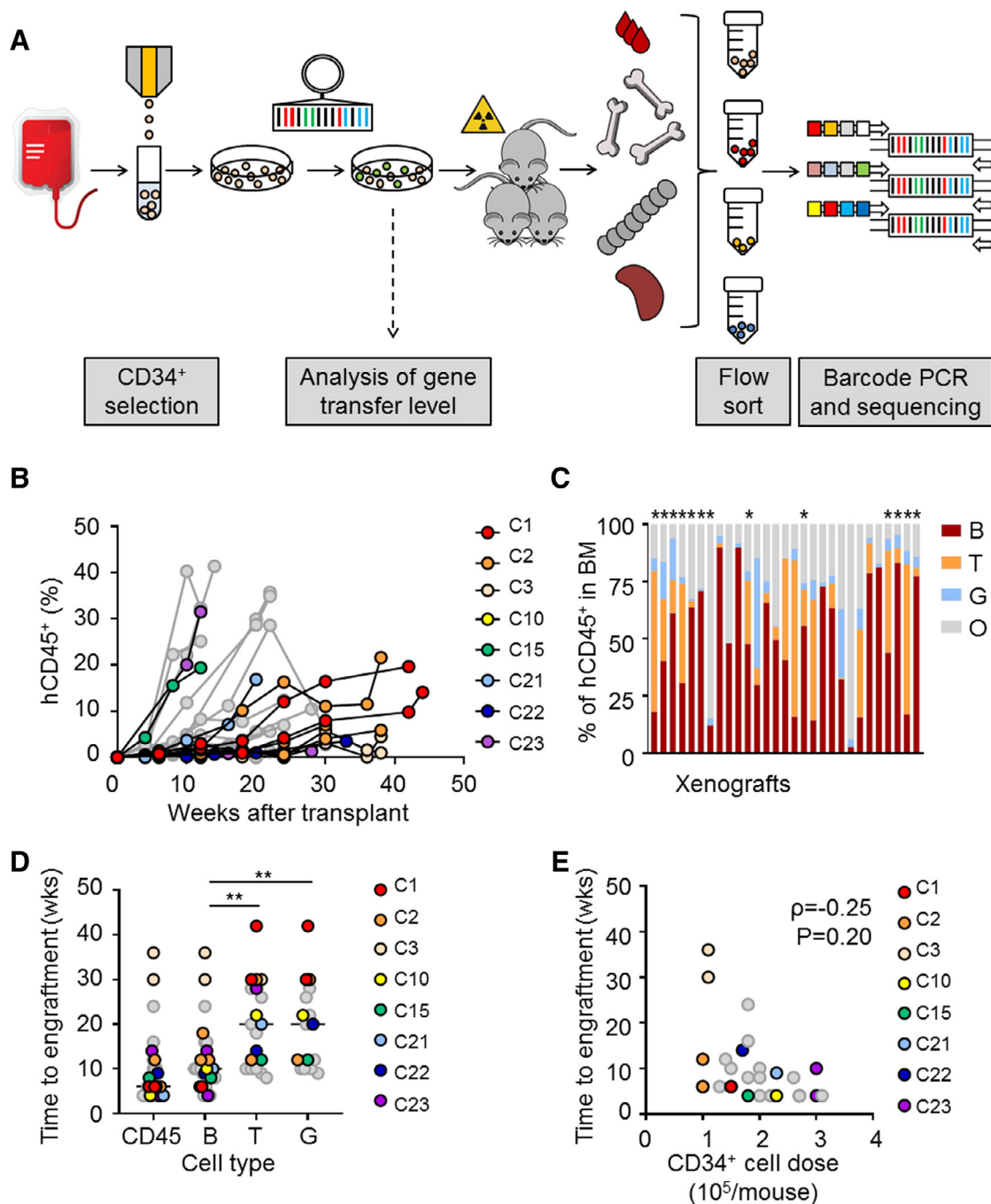


Figure 1. Engraftment and multilineage differentiation of human UCB CD34⁺ cells in murine xenografts. (A) Experimental design. Human cord blood CD34⁺ cells from 20 individual donors were isolated by positive selection using CD34 magnetic beads, followed by lentiviral cellular barcode transduction as previously described [30]. Transduction efficiency was determined by flow cytometry, after which cells were transplanted into sublethally irradiated NSG mice ($n = 30$) at a minimum dose of 1×10^5 GFP⁺ cells per recipient. Human chimerism and lineage differentiation were monitored by flow cytometry in blood throughout the experiment and in blood, bone marrow, and spleen at termination. Unsorted samples and lineage-sorted cell populations were subjected to barcode PCR, deep sequencing, and data processing as described previously [30,31]. (B) Frequency of human CD45⁺ cells (of total live peripheral blood mononuclear cells [PBMCs]) in the peripheral blood of mice over time. Connected dots represent 1 xenograft. Colors are used to depict mice engrafted with sufficient GFP⁺ cells for clone tracking using barcode analysis, as described in Figures 2 to 4. (C) Lineage commitment of human HSCs in bone marrow of murine xenografts. Each bar represents 1 mouse. Asterisks depict mice with sufficient GFP⁺ cells for barcode analysis. (D) Time to engraftment of human CD45⁺ cells, human B cells (CD45⁺/CD19⁺), human T cells (CD45⁺/CD3⁺), and human granulocytes (CD45⁺/CD16⁺). Engraftment was defined as levels above 1% of live PBMCs, which is the threshold for detection by flow cytometry. Each dot represents 1 xenograft. Colored dots represent xenografts with GFP⁺ engraftment and correspond to the data in panel C. (E) Time to human CD45⁺ cell engraftment as a function of transplanted CD34⁺ cell dose. B, B cells; T, T cells; G, granulocytes; O, other, defined as CD45⁺CD19⁻CD3⁻CD16⁻.

were more variable and generally stabilized within 16 to 20 weeks after transplantation (Figure 3B). At sacrifice, we observed a median of 12.7 (range, 4 to 167; Shannon count) clones in blood and 15.0 (range, 2 to 43) in bone marrow. The numbers of clones in blood and bone marrow of individual

recipients were highly similar and correlated with barcoded CD34⁺ cell dose (Figure 3C). Relating the number of retrieved barcodes to the administered GFP⁺CD34⁺ cell dose, we found that a median of 0.007% (range, 0.002% to 0.056%) of CD34⁺ cells produced long-term clonal progeny in our model and

Table 1
Overview of Cord Blood Samples

Donor	Barcoding Efficiency (%)	Total Cell Dose/ Mouse (10^6)	GFP ⁺ Cell Dose/ Mouse (10^6)	No. of Mice Transplanted	No. of Mice Engrafted ($\geq 1\%$ hCD45)	No. of Mice with GFP ⁺ Engraftment ($\geq 1\%$ GFP ⁺)	Lineage Engraftment ($\geq 1\%$ of hCD45 ⁺)
1	40	0.38	0.15	2	2	2	B, T, G
2	18	.50	0.10	3	3	3	B, T, G
3	30	.37	0.11	2	2	2	B, G
6	10	1.4	0.13	1	1	0	B
8	14	1.00	0.14	1	1	1*	B, G
9	11	1.36	0.15	1	1	0	B, T, G
10	7	2.89	0.23	1	1	1	B, T, G
11	8	2.86	0.22	1	1	1*	B, T, G
12	18	1.00	0.18	2	2	1*	B, T, G
13	21	0.86	0.18	1	1	0	B
14	12	2.07	0.26	1	1	0	B, T, G
15	18	1.00	0.18	1	1	1	B, G
16	13	.210	0.27	2	2	0	B, T, G
17	21	.95	0.20	2	1	0	B, T, G
18	16	1.70	0.27	2	2	0	B, T, G
19	53	0.59	0.31	1	1	0	B, T, G
20	25	0.80	0.20	2	2	0	B, G
21	65	0.35	0.23	1	1	1	B, T, G
22	81	0.21	0.17	1	1	1	B, G
23	29	1.05	0.30	2	2	1	B, T, G

Overall, 12 mice (from 8 different donors) provided enough material for reliable barcode deep sequencing. These mice are depicted in bold.

* In total, $\geq 1\%$ GFP-positive cells in bone marrow but insufficient barcode retrieval by deep sequencing.

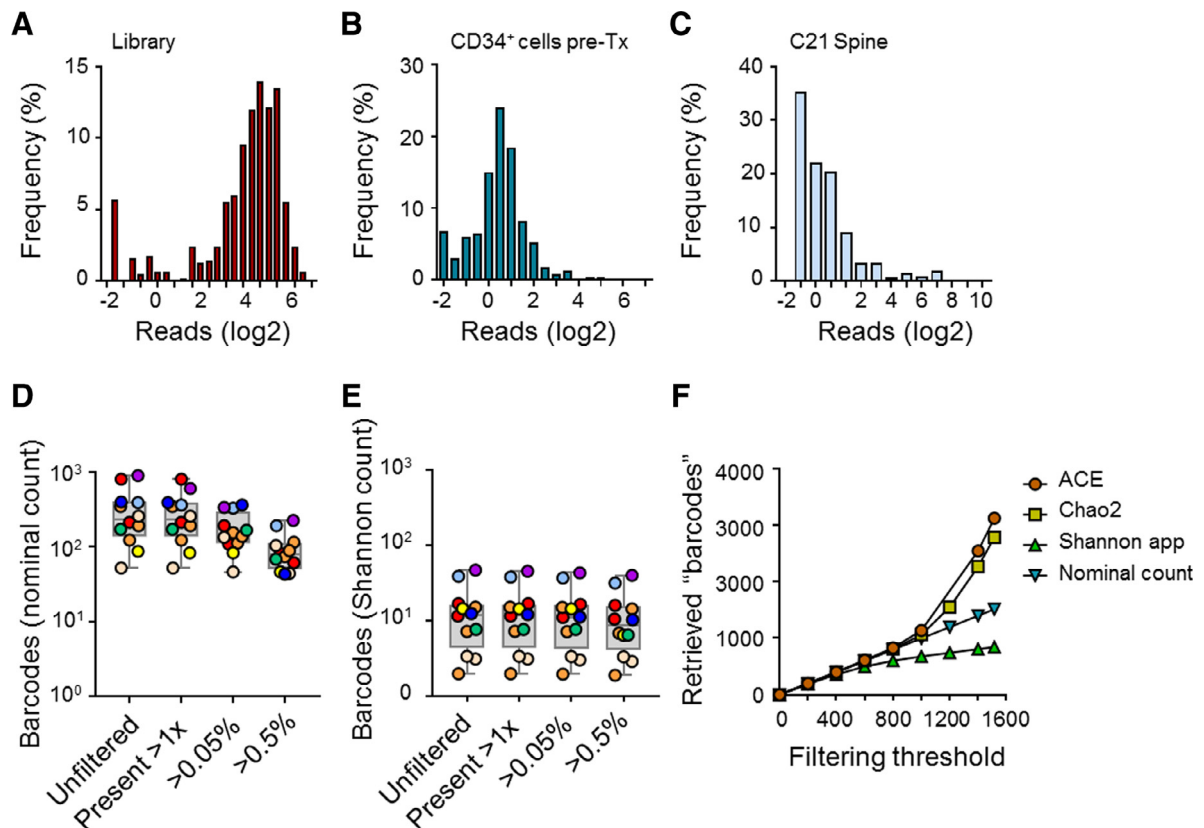


Figure 2. Impact of data analysis methods on quantification of HSPC clone numbers. (A–C) Histograms depicting barcode distribution in (A) the barcode library before target cell transduction, (B) transduced CD34⁺ cells before transplantation, and (C) a representative example of an in vivo sample from a barcoded CD34⁺ UCB xenograft. (D) Impact of data filtering on the number of retrieved HSPC clones, assessed by nominal counts. Each dot represents bone marrow of an individual UCB xenograft, and colors correspond to colors in Figure 1. (E) HSPC clone numbers in the same data set as panel D but now using the Shannon count to quantify clonal diversity. (F) Estimated barcode frequencies, using different data-filtering thresholds and estimators of diversity (for more detailed information, see Supplementary Figure S1).

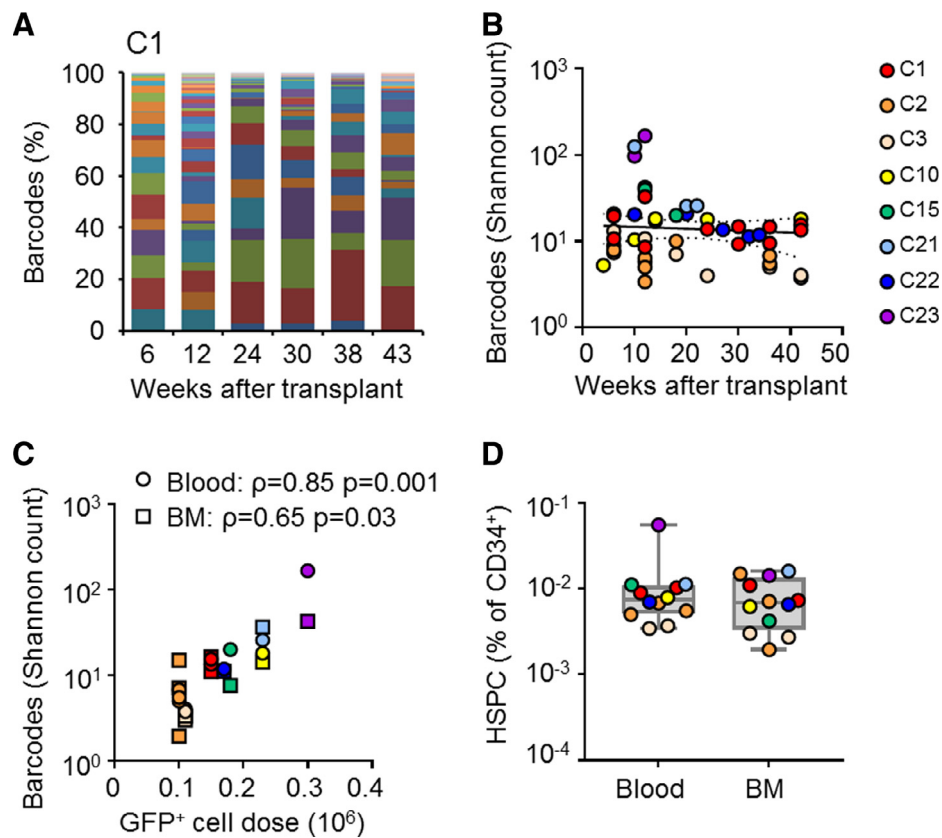


Figure 3. Frequency and interdonor variability of HSPCs among UCB CD34⁺ cells revealed by cellular barcodes. (A) Barcode composition in longitudinally obtained blood samples of a representative mouse. Each color represents an individual barcode. (B) Summary of clonal diversity in blood of 12 xenografts transplanted with 8 individual UCB donors. Xenografts transplanted from the same donor are indicated with similar colors. (C) Correlation between GFP⁺ CD34⁺ cell dose and the number of barcodes in blood (circles) and bone marrow (squares) of murine xenografts. (D) Summary of HSPC frequency, calculated by dividing the number of clones in blood or bone marrow (Shannon count), by the transplanted GFP⁺ cell dose.

that clonogenic cell frequency could vary up to 10-fold between UCB donors (Figure 3D). Notably, a higher number of clones was not significantly associated with faster donor engraftment but did correlate with increased levels of human GFP⁺CD45⁺ cells in bone marrow at sacrifice ($\rho=0.68$, $P=.02$; Supplementary Figure S3). These data indicate that the NSG-repopulating cell frequency in an enriched population of CD34⁺ UCB cells is very low and can vary up to several-fold between donors. Moreover, they suggest that early donor engraftment and long-term hematopoiesis may be mediated by distinct HSPC clones.

Initial Engraftment Is Supported by Transient Clones and Followed by Long-Term HSPCs with Stable Clonal Output

To further characterize the engraftment dynamics of individual HSPC clones, we compared clonal patterns at multiple time intervals (Figure 4). Early after transplantation, we found a relatively high number of HSPC clones in blood, many of which were small in size and transient (representative patterns in Figure 4A,B, quantification in Supplementary Figure S4). The short-term presence of these early clones was reflected by a relatively low Spearman correlation between barcode patterns in sequentially obtained blood samples at early time points (Figure 4C,D). In contrast, at later time points, the number of contributing HSPC clones became smaller and their contribution more consistent, reflected by higher Spearman correlations between barcode patterns at sequential time points (Figure 4C-E). Interestingly, the majority of HSPC clones contributing to long-term blood formation were already

present (usually as a minor clone) at the earliest time point, yet gradually grew to become dominant over time (Figure 4F and Supplementary Figure S4B). Altogether, these data demonstrate that hematopoiesis is supported by a relatively high number of transient clones early after transplant, followed by long-term hematopoiesis by a limited number of HSPCs with stable clonal output.

Most Long-Term HSPC Clones Have Multilineage Potential

To assess the lineage contribution of these long-term HSPC clones, we compared barcode patterns between sorted human cell populations from bone marrow of xenografts with robust polyclonal multilineage engraftment (C21, C22, C23; Figure 1C). Although B cells were the most abundant human cell type in the majority of xenografts, which is a known feature of the NSG model [16], we were able to isolate sufficient numbers of granulocytes and T cells for barcode analysis. The majority of HSPC clones had multilineage potential: of the top 50 most abundant barcodes in each recipient, a median of 72% (range, 32% to 100%) was found in all lineages, with varying abundance (Figure 5). Multipotent barcode clones were generally larger than lineage-restricted clones (Supplementary Figure S5), which may reflect a biological feature of multipotent clones and/or a detection issue for minor barcodes in smaller samples. Altogether, these data demonstrate that the majority of major long-term NSG-repopulating UCB CD34⁺ cells have multilineage potential, yet clones with uni- or bili-lineage potential were also present.

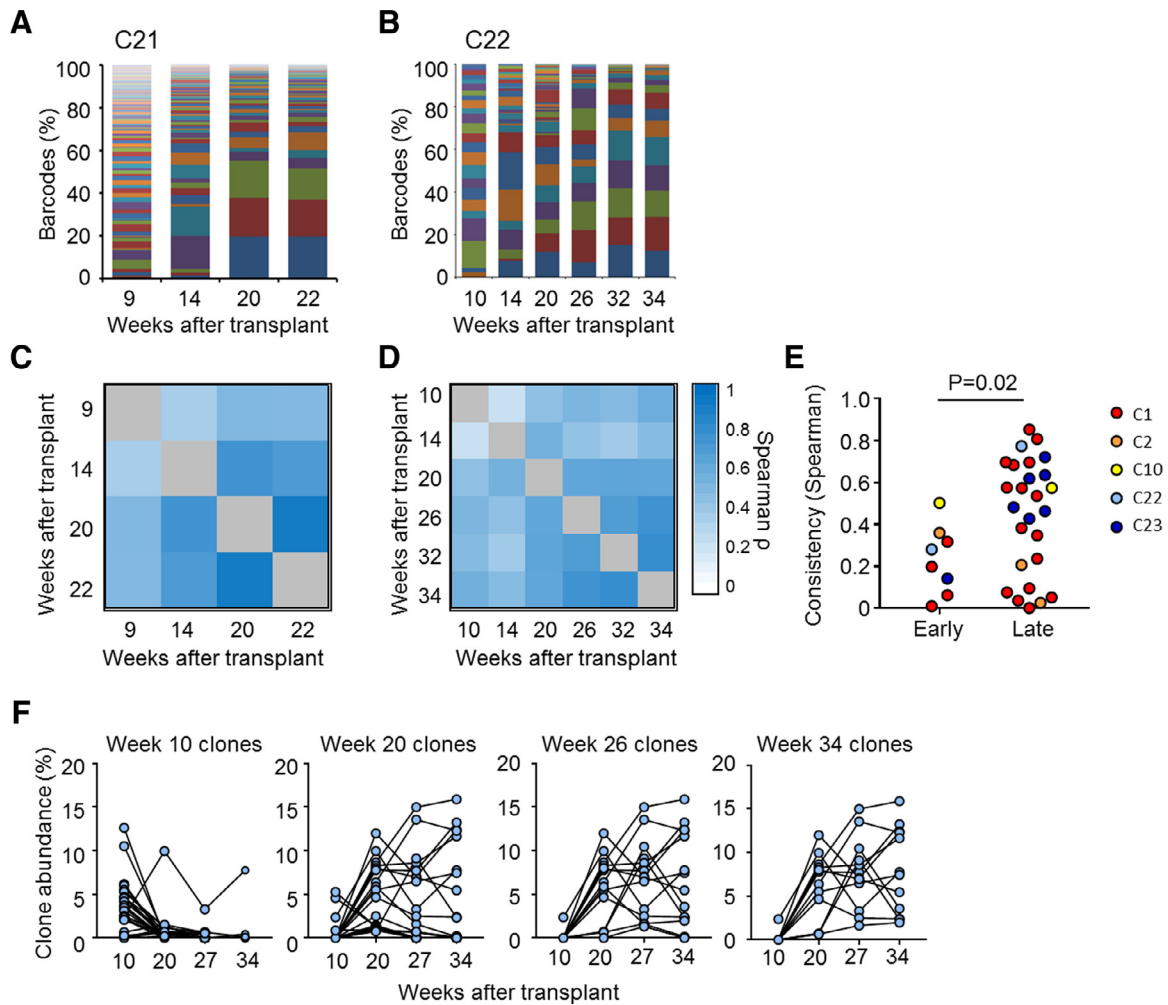


Figure 4. Blood cells are produced by transient clones early after transplantation, followed by hematopoiesis by long-term clones with stable output. (A, B) Representative examples of barcode distribution in peripheral blood of individual cord blood CD34⁺ xenografts. Each bar represents 1 time point, and colors are used to depict different barcodes. (C, D) Correlation matrix depicting Spearman correlation between barcode composition (top 100 most abundant clones) in blood drawn at different time points after transplantation. (E) Spearman correlations between blood samples drawn early after transplantation (first half of mouse life) versus those drawn at later time points (second half of mouse life). (F) Longitudinal patterns of clone sizes over time of individual barcode clones in a representative xenografts (C22). For each time point, the most abundant clones (Shannon approximation) are shown.

DISCUSSION

HSC is the only routinely used stem cell therapy in humans, which is used in over 30,000 patients annually [37]. Its success relies critically on administration of sufficient numbers of HSCs, which may be a limiting factor, especially when UCB donors are used. Very little is known about the frequency of functional long-term repopulating HSCs in UCB and how these clones behave over time. Here, we used cellular barcodes to quantitatively trace the clonal behavior of CD34⁺ HSPCs from individual UCB donors upon transplantation in murine xenografts. We demonstrate that only ~0.007% of CD34⁺ cells enriched from UCB establishes long-term progeny in murine xenografts and that this frequency can vary several-fold between different donors. Moreover, we found that quantification of clone frequencies is largely dependent on the used definitions of clonal diversity and on the analytical methods for their quantification. Altogether, our findings suggest that functional analyses and/or additional HSC markers are needed to optimize UCB donor selection protocols. In addition, as clone-tracing studies are increasingly used to understand age-related clonal hematopoiesis and the evolution of malignancy and relapse, it is of crucial importance to develop

transparent and uniform methods for HSC counting to reconcile their results.

Assessment of HSC Frequency in Human Cell Populations

In contrast to mice, in which phenotypic markers allow for the isolation and enumeration of HSCs to near purity [6], evidence regarding the phenotype and frequency of human HSCs remains controversial. Using a functional definition of HSCs and an unbiased, quantitative lineage-tracing method, we demonstrate that 0.007% of UCB CD34⁺ produces multilineage progeny in NSG mice. Our estimates are consistent with human gene therapy studies, which demonstrate that 0.001% to 0.01% of gene-corrected CD34⁺ cells has the potential to engraft long term [14,28,38]. In marked contrast, a previous barcoding study, which used pooled UCB CD34⁺ cells from >100 donors, reported HSC frequencies several-fold higher [16]. This discrepancy may be due to the *in vitro* methods for lentiviral transduction, the use of single versus multiple donors, and/or differences in the transplantation procedure [39]. In particular, in contrast to this previous study [39], we did not add any CD34⁻ competitor cells to our transplants. Although this has the advantage of preventing experimental

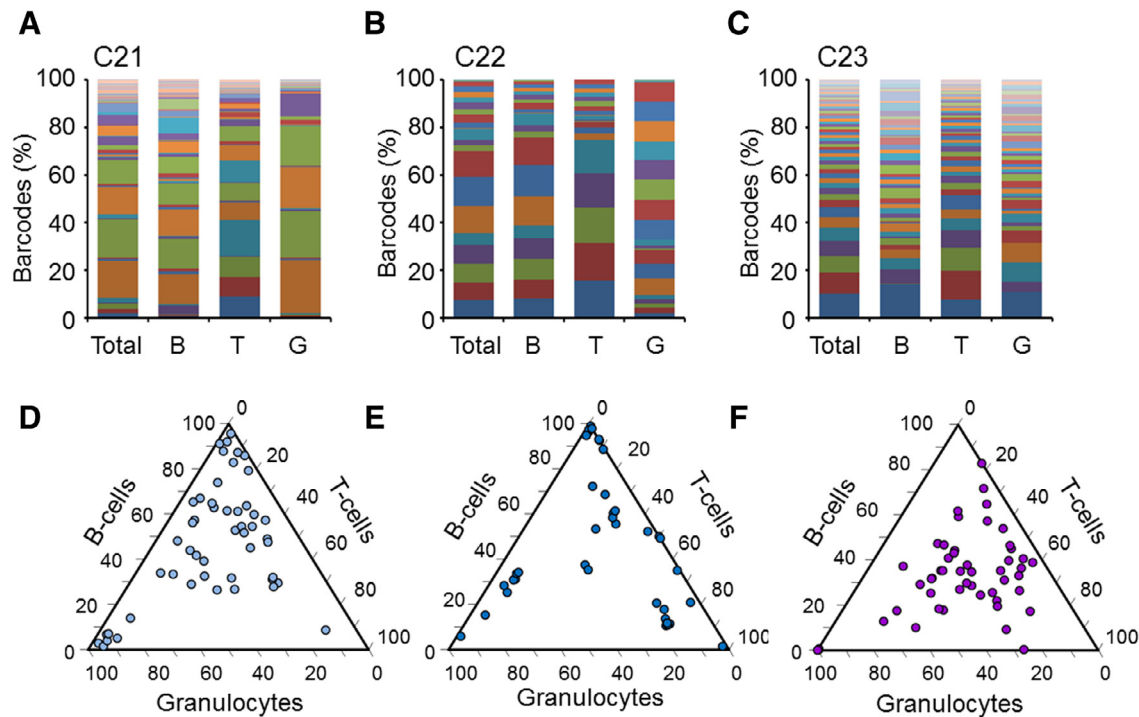


Figure 5. Multilineage engraftment of human HSPCs in murine xenografts. (A–C) Representative examples of barcode distribution in total bone marrow and in sorted B cells (CD45⁺CD19⁺), T cells (CD45⁺CD3⁺), and granulocytes (CD45⁺CD16⁺) of individual cord blood CD34⁺ xenografts. Each panel represents 1 mouse, and colors are used to depict different barcodes. (D–F) Ternary (triangle) plots of the clonal contribution of individual HSPCs to T cells, B cells, and granulocytes in bone marrow at termination of the experiments. Each dot within the triangle represents 1 individual barcode (clone).

variation due to differences in donor immunity between UCB units, the lack of donor T cells may have compromised the ability of the donor HSCs to engraft the recipient's marrow. In future, cotransplantation experiments, in which barcoded HSCs are administered together with purified CD34-negative cell populations, will be of interest to elucidate the impact of each of these populations on HSC engraftment. Moreover, in addition to these experimental differences, the analytical methods for barcode retrieval and clone counting differ markedly between these studies and have a significant impact on estimates on clonal diversity, as elaborated below.

Short-Term Progenitors Are Followed by Long-Term Multilineage HSCs

Our data are in line with previous clonal tracking studies, identifying 2 phases of post-transplant hematopoietic reconstitution [14,15,24,25,40]. The first phase is characterized by clonal instability/succession and likely reflects the output of committed progenitor cells, which may be more abundant and proliferative, yet lack the capacity to long-term self-renew. Over time, these clones are replaced by long-term multipotent HSCs, which produce stable clonal offspring for several months after transplantation. Retrospectively, we were able to detect many of these long-term clones at minor frequencies at early time points, confirming their relative quiescence compared with short-lived progenitors. The majority of long-term clones produced all blood lineages, yet clones with uni- or bilineage contribution were also found. Accordingly, the absence of granulocyte or T cell engraftment in some recipients may be due to lack of true multilineage HSCs in the graft, which may be at limiting dilution. Insight into the fundamental properties of each of these progenitor cell populations is of great interest, biologically as well as for therapeutic purposes. Can we identify phenotypic or functional markers that discriminate

long-term HSCs from transient progenitors? What are the mechanisms that guide HSC self-renewal and differentiation? How does transplantation affect HSC mutagenesis, clonal fitness, and age-related clonal hematopoiesis? In future, integrated approaches, combining genetic lineage tracing with single-cell transcriptomics [41], will provide detailed characterization of the developmental and functional properties of single human HSCs. This will contribute to better understanding of human HSC biology and may identify novel targets for increasing the number of HSCs and/or improve their long-term contribution to hematopoiesis.

Impact of Data Analysis Methods on the Number of Retrieved Clones

The large variation in reported HSPC frequencies in our study and in other clonal tracing studies in mice and men [6,8,14–16] triggered us to investigate the impact of data analysis on the number of retrieved clones. Using multiple parameters of clonal diversity on the same (filtered and unfiltered) data sets, we demonstrate that methodologic differences can cause a several-fold difference in the number of reported clones. Of all used parameters for clonal diversity, the Shannon count was the most reproducible and the least sensitive to (arbitrary) data-filtering decisions. However, most current studies, in both mice and humans, report nominal counts, either/not with correction for unseen diversity [14,16,35,36,42]. Depending on the robustness of the barcode signal and methods of data filtering, these studies may dramatically overestimate true clonal diversity. Accordingly, detailed information on sample preparation and data processing (eg, transplantation parameters, barcode calling, thresholds for noise filtering, estimators for clonal diversity) is essential for independent data interpretation, yet this is often difficult to find. To enhance reproducibility and cross-study

comparisons, guidelines for uniform and transparent reporting of data analysis decisions have been published recently [29].

To Search the Unknown: The Impact of Library Size

One factor that can greatly facilitate the reliability of barcode retrieval and noise filtering is to use a library of known complexity. Using our 800-barcode library of known content, we were able to assess commonly used strategies for data filtering and to validate the reliability of the retrieved barcodes. Importantly, we demonstrated that any overestimation of the library size greatly increases the number of false-positive barcode calls, with diversity estimates sometimes exceeding the size of the library by several-fold. Knowledge of the size of the library can thus improve data filtering significantly. However, especially for larger libraries, quantifying its exact size is not trivial, as this often relies on sequencing (part of) the library, which is subject to the same technical artifacts as described above. Here, we provide an alternative, more error-proof method of library size prediction. Using the cumulative number of unique barcodes in sequentially added samples, we observed an asymptotic increase in overall barcode diversity, which ultimately approached the size of the library. Therefore, multiple samples and/or repeated sequencing of the same samples may allow for more accurate estimation of the library size and improved data-filtering methods.

This study provides the first quantitative assessment of interdonor variation in clonogenic cell frequencies among CD34⁺ cells from different UCB donors. Our findings may (in part) explain the occurrence of nonengraftment in HSCT recipients transplanted with adequate CD34⁺ cell doses. Notably, as we only assessed a limited number of donors, true interdonor variability in UCB HSC frequency, as well as its consequences for clinical/experimental transplants, may be even larger. However, we realize that the lentiviral transduction and xenograft model may significantly affect our assessments on HSC frequency and function. In the future, innovative methods that allow for the tracing of unmanipulated HSCs in human recipients [43–45] will be needed to validate our findings. Ultimately, these studies will provide unprecedented insights into the clonal behavior of single human HSCs, which may allow for novel strategies to optimize their use in clinical HSCT and gene therapy protocols.

ACKNOWLEDGMENTS

The authors thank the midwives of the Verloskundigenpraktijk Groningen and Verloskees for collection of umbilical cord blood; H. Moes, G. Mesander, and R.J. van der Lei for their expert assistance in cell sorting; H. Schepers for assistance in the barcode transduction procedure, and R. van Os for valuable discussions.

Financial disclosure: This study was supported by research funding from the University Medical Center Groningen (Mandema Stipend to M.E.B.) and the Dutch Cancer Society (grants RUG 2014-6957 and RUG 2015-7964, both to M.E.B.).

Conflict of interest statement: There are no conflicts of interest to report.

Authorship statement: M.B., G.d.H., and L.B. designed the research. M.B., S.J., T.K., E.Z., A.A., and L.B. performed the research. M.B., E.Z., and L.B. analyzed the data. M.B., G.d.H., and L.B. wrote the manuscript.

SUPPLEMENTARY MATERIALS

Supplementary data related to this article can be found online at doi:10.1016/j.bbmt.2019.08.026.

REFERENCES

- Ballen KK, Gluckman E, Broxmeyer HE. Umbilical cord blood transplantation: the first 25 years and beyond. *Blood*. 2013;122(4):491–498.
- Wagner JE, Barker JN, DeFor TE, et al. Transplantation of unrelated donor umbilical cord blood in 102 patients with malignant and nonmalignant diseases: influence of CD34 cell dose and HLA disparity on treatment-related mortality and survival. *Blood*. 2002;100(5):1611–1618.
- Barker JN, Davies SM, DeFor T, et al. Survival after transplantation of unrelated donor umbilical cord blood is comparable to that of human leukocyte antigen-matched unrelated donor bone marrow: results of a matched-pair analysis. *Blood*. 2001;97(10):2957–2961.
- Laughlin MJ, Eapen M, Rubinstein P, et al. Outcomes after transplantation of cord blood or bone marrow from unrelated donors in adults with leukemia. *N Engl J Med*. 2004;351(22):2265–2275.
- Eapen M, Rocha V, Sanz G, et al. Effect of graft source on unrelated donor haemopoietic stem-cell transplantation in adults with acute leukaemia: a retrospective analysis. *Lancet Oncol*. 2010;11(7):653–660.
- Notta F, Doulatov S, Laurenti E, et al. Isolation of single human hematopoietic stem cells capable of long-term multilineage engraftment. *Science*. 2011;333(6039):218–221.
- Majeti R, Park CY, Weissman IL. Identification of a hierarchy of multipotent hematopoietic progenitors in human cord blood. *Cell Stem Cell*. 2007;1(6):635–645.
- Park CY, Majeti R, Weissman IL. In vivo evaluation of human hematopoiesis through xenotransplantation of purified hematopoietic stem cells from umbilical cord blood. *Nat Protoc*. 2008;3(12):1932–1940.
- Steensma DP, Bejar R, Jaiswal S, et al. Clonal hematopoiesis of indeterminate potential and its distinction from myelodysplastic syndromes. *Blood*. 2015;126(1):9–16.
- Jaiswal S, Natarajan P, Silver AJ, et al. Clonal hematopoiesis and risk of atherosclerotic cardiovascular disease. *N Engl J Med*. 2017;377(2):111–121.
- Jaiswal S, Fontanillas P, Flannick J, et al. Age-related clonal hematopoiesis associated with adverse outcomes. *N Engl J Med*. 2014;371(26):2488–2498.
- Sieburg HB, Cho RH, Dykstra B, et al. The hematopoietic stem compartment consists of a limited number of discrete stem cell subsets. *Blood*. 2006;107(6):2311–2316.
- Boztug K, Schmidt M, Schwarzer A, et al. Stem-cell gene therapy for the Wiskott-Aldrich syndrome. *N Engl J Med*. 2010;363(20):1918–1927.
- Biasco L, Pellin D, Scala S, et al. In vivo tracking of human hematopoiesis reveals patterns of clonal dynamics during early and steady-state reconstitution phases. *Cell Stem Cell*. 2016;19(1):107–119.
- Gerrits A, Dykstra B, Kalmykova OJ, et al. Cellular barcoding tool for clonal analysis in the hematopoietic system. *Blood*. 2010;115(13):2610–2618.
- Cheung AMS, Nguyen LV, Carles A, et al. Analysis of the clonal growth and differentiation dynamics of primitive barcoded human cord blood cells in NSG mice. *Blood*. 2013;122(18):3129–3137.
- Henninger J, Santoso B, Hans S, et al. Clonal fate mapping quantifies the number of haematopoietic stem cells that arise during development. *Nat Cell Biol*. 2017;19(1):17–27.
- Yu VWC, Yusuf RZ, Oki T, et al. Epigenetic memory underlies cell-autonomous heterogeneous behavior of hematopoietic stem cells. *Cell*. 2016;167(5):1310–1322. e17.
- Sykes SM, Scadden DT. Modeling human hematopoietic stem cell biology in the mouse. *Semin Hematol*. 2013;50(2):92–100.
- McKenna A, Findlay GM, Gagnon JA, et al. Whole-organism lineage tracing by combinatorial and cumulative genome editing. *Science*. 2016;353(6298):aaf7907.
- Pei W, Feyerabend TB, Rössler J, et al. Polylox barcoding reveals haematopoietic stem cell fates realized in vivo. *Nature*. 2017;548(7668):456–460.
- Verovskaya E, Broekhuis MJC, Zwart E, et al. Heterogeneity of young and aged murine hematopoietic stem cells revealed by quantitative clonal analysis using cellular barcoding. *Blood*. 2013;122(4):523–532.
- Lu R, Neff NF, Quake SR, Weissman IL. Tracking single hematopoietic stem cells in vivo using high-throughput sequencing in conjunction with viral genetic barcoding. *Nat Biotechnol*. 2011;29(10):928–933.
- Naik SH, Perié L, Swart E, et al. Diverse and heritable lineage imprinting of early haematopoietic progenitors. *Nature*. 2013;496(7444):229–232.
- Wu C, Espinoza DA, Koelle SJ, et al. Geographic clonal tracking in macaques provides insights into HSPC migration and differentiation. *J Exp Med*. 2017;215(1):217–232.
- Wu C, Li B, Lu R, et al. Clonal tracking of rhesus macaque hematopoiesis highlights a distinct lineage origin for natural killer cells. *Cell Stem Cell*. 2014;14(4):486–499.
- Aiuti A, Biasco L, Scaramuzza S, et al. Lentiviral hematopoietic stem cell gene therapy in patients with Wiskott-Aldrich syndrome. *Science*. 2013;341(6148):1233451.
- Aiuti A, Slavin S, Aker M, et al. Correction of ADA-SCID by stem cell gene therapy combined with nonmyeloablative conditioning. *Science*. 2002;296(5577):2410–2413.
- Lyne A-M, Kent DG, Laurenti E, et al. A track of the clones: new developments in cellular barcoding. *Exp Hematol*. 2018;68:15–20.

30. Belderbos ME, Koster T, Ausema B, et al. Clonal selection and asymmetric distribution of human leukemia in murine xenografts revealed by cellular barcoding. *Blood*. 2017;129(24):3210–3220.
31. Bystrykh LV, Belderbos ME. Clonal analysis of cells with cellular barcoding: when numbers and sizes matter. *Methods Mol Biol*. 2016;1516:57–89.
32. Radtke S, Adair JE, Giese MA, et al. A distinct hematopoietic stem cell population for rapid multilineage engraftment in nonhuman primates. *Sci Transl Med*. 2017;9(414):eaan1145.
33. Chao A, Colwell RK, Lin C-W, Gotelli NJ. Sufficient sampling for asymptotic minimum species richness estimators. *Ecology*. 2009;90(4):1125–1133.
34. Chao A, Bunge J. Estimating the number of species in a stochastic abundance model. *Biometrics*. 2002;58(3):531–539.
35. De Ravin SS, Wu X, Moir S, et al. Lentiviral hematopoietic stem cell gene therapy for X-linked severe combined immunodeficiency. *Sci Transl Med*. 2016;8(335):335ra57.
36. Cooper AR, Lill GR, Shaw K, et al. Cytoablative conditioning intensity predicts clonal diversity in ADA-SCID retroviral gene therapy patients. *Blood*. 2017;129(19):2624–2635.
37. Li HW, Sykes M. Emerging concepts in haematopoietic cell transplantation. *Nat Rev Immunol*. 2012;12(6):403–416.
38. Boitano AE, Wang J, Romeo R, et al. Aryl hydrocarbon receptor antagonists promote the expansion of human hematopoietic stem cells. *Science*. 2010;329(5997):1345–1348.
39. Nguyen LV, Pellacani D, Lefort S, et al. Barcoding reveals complex clonal dynamics of de novo transformed human mammary cells. *Nature*. 2015;528(7581):267–271.
40. Dykstra B, Olthof S, Schreuder J, Ritsema M, de Haan G. Clonal analysis reveals multiple functional defects of aged murine hematopoietic stem cells. *J Exp Med*. 2011;208(13):2691–2703.
41. Kester L, Van Oudenaarden A. Cell stem cell review single-cell transcriptomics meets lineage tracing. *Stem Cell*. 2018;23:166–179.
42. Ott MG, Schmidt M, Schwarzwaelder K, et al. Correction of X-linked chronic granulomatous disease by gene therapy, augmented by insertional activation of MDS1-EVI1, PRDM16 or SETBP1. *Nat Med*. 2006;12(4):401–409.
43. Alemany A, Florescu M, Baron CS, Peterson-Maduro J, van Oudenaarden A. Whole-organism clone tracing using single-cell sequencing. *Nature*. 2018;556(7699):108–112.
44. Osorio FG, Rosendahl Huber A, Oka R, et al. Somatic mutations reveal lineage relationships and age-related mutagenesis in human hematopoiesis. *Cell Rep*. 2018;25(9):2308–2316.e4.
45. Behjati S, Huch M, van Boxtel R, et al. Genome sequencing of normal cells reveals developmental lineages and mutational processes. *Nature*. 2014;513(7518):422–425.